Stability and Dissipation of Laminar Vortex Flow in Superfluid ^{3}He-B

V. B. Eltsov,[1,2] R. de Graaf,[1] P. J. Heikkinen,[1] J. J. Hosio,[1] R. Hänninen,[1] M. Krusius,[1] and V. S. L'vov[3]

[1]*Low Temperature Laboratory, School of Science and Technology, Aalto University, Finland*

[2]*Kapitza Institute for Physical Problems, Kosygina 2, 119334 Moscow, Russia*

[3]*Department of Chemical Physics, The Weizmann Institute of Science, Rehovot 76100, Israel*

(Received 3 May 2010; revised manuscript received 9 August 2010; published 14 September 2010)

A central question in the dynamics of vortex lines in superfluids is dissipation on approaching the zero temperature limit $T \to 0$. From both NMR measurements and vortex filament calculations, we find that vortex flow remains laminar up to large Reynolds numbers $\mathrm{Re}_\alpha \sim 10^3$ in a cylinder filled with ^{3}He-B. This is different from viscous fluids and superfluid ^{4}He, where the corresponding responses are turbulent. In ^{3}He-B, laminar vortex flow is possible in the bulk volume even in the presence of sizable perturbations from axial symmetry to below $0.2T_c$. The laminar flow displays no excess dissipation beyond mutual friction, which vanishes in the $T \to 0$ limit, in contrast with turbulent vortex motion where dissipation has been earlier measured to approach a large T-independent value at $T \lesssim 0.2T_c$.

DOI: 10.1103/PhysRevLett.105.125301 PACS numbers: 67.30.hb, 02.70.Pt, 47.15.ki, 67.30.he

For centuries, the transition to turbulence has been one of the enigmatic unsolved problems of classical hydrodynamics. It is commonly accepted that laminar flow becomes unstable with increasing Reynolds number Re_ν above some case-dependent threshold. In special geometries, particularly in a circular pipe, laminar flow is assumed asymptotically stable with respect to infinitesimal perturbations at any Re_ν [1], but the critical amplitude of perturbation, which triggers turbulence, decreases rapidly as $\propto 1/\mathrm{Re}_\nu$ [2]. In practice, normal fluid flows are thus turbulent at sufficiently high Re_ν.

What can be said about the transition to turbulence in the flow of vortices in superfluids? When $T \to 0$, dissipation from mutual friction approaches zero and laminar vortex flow is believed to become unstable. This is the current impression about 3-dimensional vortex flow in superfluid ^{4}He. Here we show that in superfluid ^{3}He-B laminar vortex flow is stable to below $0.20T_c$ in an axially symmetric situation, and, to make it turbulent, a strong perturbation is needed. The laminar bulk volume response is associated with mutual friction only, and, since it does not support vortex reconnections, this suggests that the $T \to 0$ dissipation measured earlier [3,4] for turbulent vortex flow is powered by reconnections.

Laminar flow.—The Reynolds number $\mathrm{Re}_\nu \equiv VL/\nu$ provides an estimate of the ratio of the inertial ($\sim V^2/L$) and dissipative ($\sim \nu V/L^2$) terms in the Navier-Stokes equation, via the kinematic viscosity of the fluid ν and the typical velocity and length scales V and L, respectively [5,6]. Phenomenologically, superfluids are described as a mixture of the superfluid and normal components with separate velocities $\boldsymbol{v}_s$ and $\boldsymbol{v}_n$, densities ρ_s and ρ_n, and viscosities $\nu_s \equiv 0$ and $\nu_n > 0$. The equation for $\boldsymbol{v}_s(\boldsymbol{r}, t)$ is similar to the inviscid Euler equation [7]:

$$\frac{\partial \boldsymbol{v}_s}{\partial t} + (\boldsymbol{v}_s \cdot \boldsymbol{\nabla})\boldsymbol{v}_s + \boldsymbol{\nabla}\mu = -\alpha' \tilde{\boldsymbol{v}}_s \times \boldsymbol{\omega}_s + \alpha \hat{\boldsymbol{\omega}} \times [\boldsymbol{\omega}_s \times \tilde{\boldsymbol{v}}_s], \quad (1)$$

but with additional terms ($\propto \tilde{\boldsymbol{v}}_s \equiv \boldsymbol{v}_s - \boldsymbol{v}_n$) on the right-hand side, which describe the dissipative ($\propto \alpha$) and reactive ($\propto \alpha'$) mutual friction between the normal and superfluid components, mediated by the superfluid vorticity $\boldsymbol{\omega}_s = \boldsymbol{\nabla} \times \boldsymbol{v}_s$. Here μ is the chemical potential and $\hat{\boldsymbol{\omega}} = \boldsymbol{\omega}_s/\omega_s$. By setting $\boldsymbol{v}_n = 0$, the ratio of the inertial and dissipative terms in Eq. (1) can be understood as the superfluid Reynolds number [8]

$$\mathrm{Re}_\alpha(T) \equiv [1 - \alpha'(T)]/\alpha(T). \quad (2)$$

It is independent of velocity, determined only by the temperature dependence of α and α'. Since these decrease rapidly in the limit $T \to 0$, where $\mathrm{Re}_\alpha \to 1/\alpha \gg 1$, superfluid dynamics is expected to become turbulent.

This is the case in superfluid ^{4}He, where turbulence at the lowest temperatures is ubiquitous in measurements with moving vortices, including so-called *spin-up* or *spin-down* measurements, where a sudden change is applied to the angular velocity $\Omega(t)$ of the rotating cryostat (see Ref. [9] for measurements on a cylinder or Ref. [10] on a cube). For simplicity, the step change is usually applied from 0 to some Ω or from Ω to 0. Independently of the shape of the container, in experimental work [9,10] the turbulent response of the superfluid component has been interpreted as the creation of a turbulent Ekman boundary layer, which expands toward the center of the container. This is similar to what happens in rotating viscous fluids [5]. In short, the transition to turbulent vortex flow in superfluid ^{4}He generally resembles that in viscous fluids.

^{3}He-B appears to behave differently: Our noninvasive NMR measurements show that in a cylinder spin down is

laminar even at $0.2T_c$ and $\mathrm{Re}_\alpha \sim 10^3$. The same applies for spin up in specially prepared situations below $0.3T_c$. In contrast, the response is turbulent when two quartz tuning fork sensors inside the cylinder obstruct cylindrically symmetric flow. In the low temperature limit, where the transport of normal excitations is ballistic, the main difference of ^{3}He-B from ^{4}He is a much larger vortex core radius, $a \sim 10$–80 nm. Thus the stability of laminar flow and the transition to turbulence depend on the quantum properties of these two superfluids.

In a long cylinder, oriented parallel to the rotation axis, laminar rotating flow of the superfluid component is solid-body-like, $\langle \boldsymbol{v}_s \rangle = \boldsymbol{\Omega}(t) \times \boldsymbol{r}$, confined to the azimuthal plane. This requires that vortex lines are highly polarized along the cylinder axis and their motion is predominantly 2-dimensional along spirally contracting (spin-up) or expanding (spin-down) trajectories in the azimuthal plane. The motion is obtained from Eq. (1), which simplifies in terms of its radial dependence to

$$\frac{d\Omega(t)}{dt} = 2\alpha\Omega(t)[\Omega_r - \Omega(t)]. \tag{3}$$

We apply a step change in rotation at $t = 0$ and follow the spin-down response $\Omega_\Downarrow(t)$ from Ω_0 while the rotation drive is $\Omega_r = 0$ (or the spin-up response $\Omega_\Uparrow(t)$ from $\varepsilon\Omega_0$ while the drive is $\Omega_r = \Omega_0$). This gives the solutions

$$\Omega_\Downarrow(t) = \Omega_0/[1 + t/\tau_\Downarrow], \tag{4a}$$

$$\Omega_\Uparrow(t) = \varepsilon\Omega_0/[\varepsilon + (1 - \varepsilon)\exp(-t/\tau_\Uparrow)], \tag{4b}$$

$$\tau = \tau_\Downarrow(T) = \tau_\Uparrow(T) = [2\alpha(T)\Omega_0]^{-1}. \tag{4c}$$

Thus laminar vortex flow corresponds to a monotonic response of $\langle \boldsymbol{v}_s \rangle$ and of the total vortex length L towards the final state. This is to be distinguished from a turbulent response where L first builds up to an overshoot and then relaxes faster than in the laminar case.

Measurement.—The vortex flow response is recorded with noninvasive NMR techniques in a smooth-walled quartz cylinder of 6 mm diameter. The 110 mm long NMR section is separated with a flat division wall and a small orifice from the rest of the cylinder, which houses two quartz tuning fork oscillators for thermometry [4]. The cylinder is aligned along the rotation axis within $\lesssim 1°$. Established procedures exist for preparing the NMR volume in a state of vortex-free counterflow (cf), where the normal component is in solid-body rotation and the superfluid at rest. This gives rise to a so-called cf peak in the NMR absorption spectrum. We use it to measure the spin-up and spin-down responses [4]. Its height and shift from the Larmor frequency f_L are functions of the azimuthal large-scale cf and are calibrated experimentally at different values of constant rotation Ω in the vortex-free state, as seen in Fig. 1(a).

Figure 1(b) shows an example of the decay of the cf peak during spin down and spin up, as expressed via the equivalent Ω from the calibration plot in Fig. 1(a). During the initial rapid change of the drive $\Omega(t)$ (at $|\dot{\Omega}| = 0.03$ rad/s^2), the cf peak grows continuously and reaches maximum height at $t = 0$ when the final constant value of drive is attained. From there on the peak decreases monotonically, obeying the solid-body cf properties of the calibration. Deviations from the calibrated peak height versus frequency dependence would indicate that the laminar flow state is changing, e.g., from turbulent tangling. Should the polarization along the cylinder axis be entirely lost because of turbulence, then the cf peak would disappear and the absorption would be shifted to a broad maximum close to f_L. Note that the integrated absorption in the NMR spectrum is a constant at a given temperature. Thus a shift of absorption from the cf peak to other frequencies would be

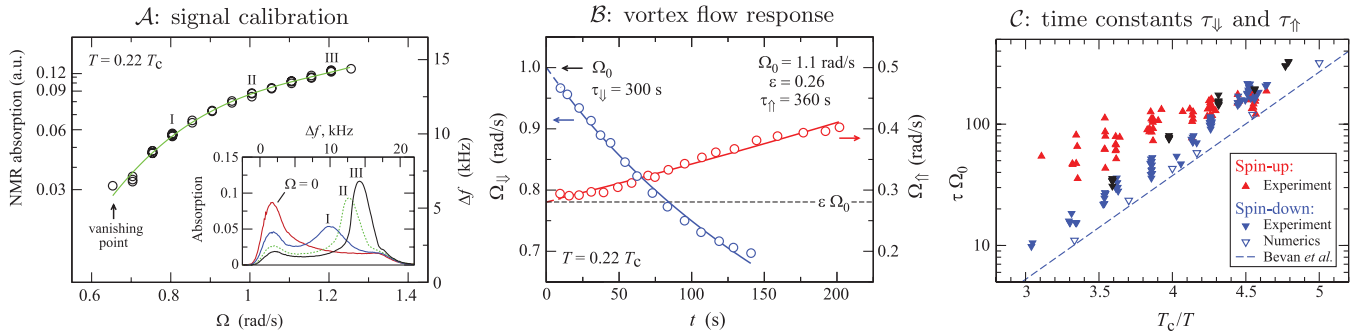

FIG. 1 (color). NMR measurement of spin down and spin up at 29 bar pressure. (Left) Calibration of the cf peak in the NMR absorption spectrum in *vortex-free rotation* at $0.22T_c$. The peak height is plotted on the left vertical axis, its shift $\Delta f = f_{\mathrm{cf}} - f_L$ from the Larmor frequency $f_L = 1.97$ MHz on the right axis, and the corresponding drive Ω at constant rotation on the bottom axis. In the inset examples of NMR spectra are shown. (Middle) Spin-down and spin-up responses plotted versus time. By using the calibration in panel $\mathcal{A}$, the heights and/or frequency shifts of the cf peak during its decay have been converted to corresponding Ω values. The results have been fitted to Eqs. (4a) and (4b), to extract the characteristic times $\tau_\Downarrow$ and $\tau_\Uparrow$ in Eq. (4c). The extrapolation of the fits to $t = 0$ gives Ω_0 for spin down or $\varepsilon\Omega_0$ for spin up. (Right) Characteristic spin-down and spin-up times given in terms of $\Omega_0\tau = 1/(2\alpha)$ versus normalized inverse temperature T_c/T: Our measurements of $\tau(T)$ (filled triangles) are compared to $1/(2\alpha)$ extrapolated from data on $\alpha(T)$ measured above $0.35T_c$ in Ref. [11] (dashed line) and to the calculated spin down in the cylinder with $\eta = 2°$, which uses the mutual friction from Ref. [11] (open triangles).

seen as a *faster* decay of the azimuthal flow. We conclude that the slow and continuous cf absorption response can result only from smoothly decaying azimuthal global flow and proves the laminar nature of the vortex flow state.

Figure 1(c) shows the characteristic decay time τ of laminar vortex flow as a function of inverse temperature from measurements in the rotation range 0.7–2.5 rad/s. The data agree well with earlier measurements [11] of dissipative mutual friction $\alpha(T)$, considering that temperature measurement in the two experiments also carries uncertainties. Spin-up times are longer, which is not expected from Eq. (4c) but can be explained by the additional time required for generating new vortices. The spin-up model in Eq. (4b) assumes an instantaneous ample supply of remanent vortices, which cover homogeneously the cylindrical wall. This requires that a spin-up measurement is performed soon after a previous spin-down run, or else the remanent vortices are reduced to a few and spin up starts from a localized vortex formation event, followed by axial vortex motion with a propagating turbulent front [4]. In conclusion, the response times in Fig. 1(c) constitute the first observations of laminar spin up and spin down, which remain stable with no additional dissipation beyond the mutual friction from radial vortex motion, up to large $\mathrm{Re}_\alpha \sim 10^3$.

Numerical simulation.—To shed more light on the laminar vortex response, we use vortex filament calculations [12]. Since vortex creation is problematic in spin-up calculations, only spin down will be considered.

Spherical container: Fig. 2(a).—The insets show top and side views of calculated vortex configurations, which expand in time during laminar spin down, with individual vortices moving along spiral trajectories to the equatorial wall, where they finally annihilate as half rings with a radius comparable to the core diameter. During all evolution the configuration is smoothly laminar, with no sign of tangling. This case resembles a decelerating rotating neutron star [13] and represents a most symmetric flow environment.

Circular cylinder: Fig. 2(b).—To mimic a small perturbation from axial symmetry and to break translational invariance along the rotation axis, we tilted the cylinder by $\eta = 2°$ from the rotation axis [12]. Thus initially at $t = 0$ the vortices are slightly inclined with respect to the cylinder. This aberration is small, the vortices are almost rectilinear, of equal length, and their density is constant, $2\Omega(0)/\kappa$, as required for solid-body rotation [see top view in the leftmost inset; $\kappa = h/(2m_3)$ is the circulation quantum]. The inset in the middle shows the top view a little later, when vortices in the outermost ring have partly reconnected at the cylindrical wall, are of reduced length, and are gradually annihilating. Meanwhile, vortices inside the outer ring have changed only a little in shape. Much later (top and side views, rightmost insets) the remaining vortices are still evenly distributed and smooth on the scale of the intervortex distance ℓ.

In the main panel in Fig. 2(b), the calculated total vortex length $L(t)$ has been fitted to the spin-down dependence of Eq. (4a). This yields the $\tau_\Downarrow$ values shown in Fig. 1(c), which are in good agreement with our measurements. The mean polarization remains continuously high, $p_z(t) > 0.95$, which applies for all temperatures $\geq 0.20T_c$, but, in particular, at 0.2–$0.3T_c$ $p_z(t)$ does not change with temperature. The total number of reconnections on the cylindrical wall, $N_s(\infty)$, is 3 times larger than the initial number

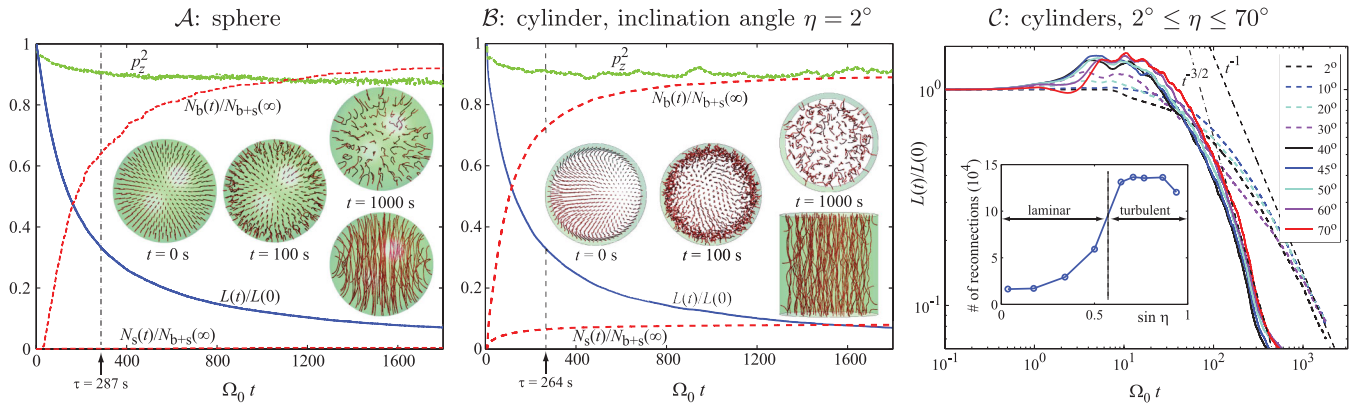

FIG. 2 (color). Numerical calculations of spin down with $\Omega_0 = 0.5$ rad/s, $\alpha = 4.3 \times 10^{-3}$, and $\alpha' = 9.1 \times 10^{-5}$ (which corresponds to $0.22T_c$ and 29 bar). (Left) Sphere of radius 3 mm; prepared to be initially in the equilibrium vortex state with $\mathcal{N}(0) = \mathcal{N}_{\mathrm{eq}}(\Omega_0) = 325$ vortices; total number of vortex reconnections in the bulk $N_b(\infty) \approx 740$ and with the container surface $N_s(\infty) \approx 4$. The normalized curves in the main panel represent: (a) calculated total vortex length $L(t)/L(0)$ [indistinguishable from a fit to Eq. (4a) yielding $\tau_\Downarrow = 287$ s]—solid (blue) curve; (b) mean vortex polarization along the symmetry axis of the container $\langle p_z^2 \rangle$—dotted (green) curve; (c) cumulative number of vortex reconnections in the bulk $N_b(t)/[N_b(\infty) + N_s(\infty)]$ and on the surface $N_s(t)/[N_b(\infty) + N_s(\infty)]$—dashed (red) curves. Insets: Top views at $t = 0$ and 100 s; top and side views at $t = 1000$ s. (Middle) Cylinder with diameter = height = 6 mm; inclined by $\eta = 2°$ from the rotation axis; $\mathcal{N}(0) = \mathcal{N}_{\mathrm{eq}}(\Omega_0) = 413$, $N_b(\infty) \approx 15\,000$, and $N_s(\infty) \approx 1400$. (Right) The same cylinder at different inclination angles η. The time dependence of $L(t)/L(0)$ is plotted on logarithmic scales. The overall flow behavior is laminar for $\eta \lesssim 30°$ and turbulent for $\eta \gtrsim 40°$. Inset: Total number of all reconnections as a function of inclination η displaying a sharp increase at the hydrodynamic transition.

of vortices, $\mathcal{N}(0)$. This suggests that vortex annihilation is facilitated in the tilted cylinder by reconnections with the cylindrical wall. Reconnections in the bulk volume are 10 times more abundant but occur in the outermost ring of vortices; i.e., reconnections are limited to a turbulent boundary layer. At $0.20T_c$ it has a width $\sim\ell$, which decreases with increasing temperature so that at $0.30T_c$ only wall reconnections remain [14]. Thus this numerical example is consistent with our measurements and the claim that laminar spin down is stable in the bulk volume with respect to a finite-size perturbation even at large Re_α.

Tilted cylinder: Fig. 2(c).—By varying the inclination η, we introduce a controllable perturbation. It forces the superfluid to adjust to the elliptically distorted boundary condition and to edge effects at the tilted top and bottom surfaces of the cylinder. This makes it possible to identify a transition from laminar to turbulent spin down from the time dependence of $L(t)$ with increasing η. When $\eta \lesssim 30°$, $L(t)$ displays no or a minor overshoot and is followed by a slow falloff with t^{-1} dependence, as obtained for laminar flow in Eq. (4a). When $\eta \gtrsim 40°$, the overshoot grows larger and the spin-down decay falls on the faster $t^{-3/2}$ dependence, typical for turbulent flow [15].

The overshoot in $L(t)$ arises when vortices reconnect in the bulk volume and form a turbulent tangle. Here the polarization along the rotation axis is largely lost, and the kinetic energy of the global azimuthal flow is converted to an increase in vortex density via frequent reconnections. The increase in reconnections [inset in Fig. 2(c)] is associated with an expansion of the turbulent boundary layer to an almost even radial distribution of reconnections. Simultaneously, small-scale structure appears on the vortices, when the mean curvature radius decreases with η. These features characterize the turbulent overall evolution, although the turbulence is not homogeneous but concentrates towards large radii. The large inclination $\eta \sim 30°$–$40°$, which is required to turn the overall spin-down response turbulent, underlines the robustness of laminar flow in a cylindrically symmetric environment.

Cubic container.—The turbulent signatures are also displayed by calculations on a cube of similar size [16]. The total number of reconnections is here an order of magnitude larger than in Fig. 2(b). After an initial 50% overshoot in $L(t)$, the decay can be fitted with $L(t)/L(0) \propto (1 + t/\tau)^{-3/2}$, where $\tau = 70$ s at $0.22T_c$.

Kelvin wave excitations.—In Fig. 2(b), one can see bending of vortex lines which can be interpreted as Kelvin waves (KWs). To clarify the role of KWs during spin down in the weakly tilted cylinder, compare the kinetic energy (per unit mass) of laminar rotation $E_{\mathrm{HD}} = (\Omega R)^2/4$ with the KW energy $E_{\mathrm{KW}} \simeq \Lambda\kappa\Omega(1 - \langle p_z^2\rangle)/2$, where $\Lambda \equiv \ln(\ell/a) \simeq 10$ in ^{3}He-B. One finds

$$E_{\mathrm{KW}}/E_{\mathrm{HD}} \approx 4\Lambda(1 - \langle p_z^2\rangle)/\mathcal{N}. \quad (5)$$

The polarization is $\langle p_z^2\rangle \simeq 0.9$, the number of vortices $\mathcal{N} \sim 400$–40 during the evolution shown in Fig. 2(b), and thus $E_{\mathrm{KW}}/E_{\mathrm{HD}} \sim 0.015$–$0.15$ and is not changing with temperature, according to the simulation results. This means that KWs practically do not contribute to the total energy. A second argument is derived by comparing dissipation of KWs via mutual friction and the nonlinear KW-energy cascade [17]. The cascade may develop only if $\alpha\Lambda \ll (1 - \langle p_z^2\rangle)^4$, which is not the case here. We conclude that KWs play no role in the total energy loss, which is consistent with the experimental result.

Conclusions.—In a rotating cylinder, vortex flow responses can be laminar in the absence of strong flow perturbations and surface pinning at the lowest temperatures. The measured decay time is exclusively accounted for by radial vortex motion, damped by the exponentially vanishing mutual friction dissipation. The distinctive feature of such laminar flow is a low incidence of vortex reconnections and of Kelvin wave excitations in the bulk volume. At $0.20T_c$ the dissipation is 2 orders of magnitude lower than in the axially inhomogeneous spin up in the form of a propagating turbulent vortex front [4]. This remarkable difference suggests that turbulent dissipation in the $T \to 0$ limit is excited by vortex reconnections.

This work is supported by the Academy of Finland, the EU FP7 Microkelvin program, and the U.S.–Israel Binational Science Foundation.

[1] B. Hof *et al.*, Phys. Rev. Lett. **101**, 214501 (2008).
[2] B. Hof, A. Juel, and T. Mullin, Phys. Rev. Lett. **91**, 244502 (2003).
[3] D. I. Bradley *et al.*, Phys. Rev. Lett. **96**, 035301 (2006).
[4] V. B. Eltsov *et al.*, Phys. Rev. Lett. **99**, 265301 (2007).
[5] H. P. Greenspan, *The Theory of Rotating Fluids* (Cambridge University Press, Cambridge, England, 1968).
[6] P. G. Drazin and W. H. Reid, *Hydrodynamic Stability* (Cambridge University Press, Cambridge, England, 1980).
[7] E. B. Sonin, Rev. Mod. Phys. **59**, 87 (1987).
[8] A. P. Finne *et al.*, Nature (London) **424**, 1022 (2003).
[9] P. W. Adams, M. Cieplak, and W. I. Glaberson, Phys. Rev. B **32**, 171 (1985).
[10] P. Walmsley *et al.*, Phys. Rev. Lett. **99**, 265302 (2007).
[11] T. D. C. Bevan *et al.*, J. Low Temp. Phys. **109**, 423 (1997).
[12] R. Hänninen, J. Low Temp. Phys. **156**, 145 (2009).
[13] Turbulence in a decelerating neutron star is frequently discussed; see, e.g., G. Greenstein, Nature (London) **227**, 791 (1970); N. Andersson *et al.*, Mon. Not. R. Astron. Soc. **381**, 747 (2007).
[14] The calculations have been performed with a resolution which spatially is of order 0.1 mm and temporally 0.02 s. The quoted reconnection numbers are rather insensitive to the numerical grid spacings at this level of resolution.
[15] Dissipation in turbulent decay is often expressed as an effective kinematic viscosity ν', which proves to be 0.02κ (tilted cylinder, $\eta \geq 40°$) and 0.03κ (cube, $\eta = 2°$).
[16] More material: http://ltl.tkk.fi/~rhannine/spindown/.
[17] V. L'vov and S. Nazarenko, Pis'ma Zh. Eksp. Teor. Fiz. **91**, 464 (2010).